Theory of nonlinear ballistic transport in quasi-one-dimensional constrictions

Hongqi Xu
*Department of Solid State Physics, University of Lund, Box 118, S-221 00 Lund, Sweden**
and Department of Physics and Measurement Technology, Linköping University, S-581 83 Linköping, Sweden
(Received 12 January 1993)

We report on quantum-mechanical calculations of the differential conductance G of a ballistic and uniform constriction in the nonlinear-response regime of transport. The constriction has been connected to two semi-infinite two-dimensional electron gases, which serve as emitter and collector when a source-drain voltage V_{sd} is applied. In accordance with the fact that there should not be any electron backscatterings in the idealized constriction, it is assumed, in the calculations, that the electrostatic potential is flat in the constriction along the transport direction and the voltage drops of the applied source-drain voltage occur only at the ends of the constriction. Our calculations show that in addition to the conductance plateaus, which are quantized at multiples of $2e^2/h$ in the linear-response regime of transport, new plateau structure develops as the source-drain voltage is increased. We predict that the edges of the conductance plateaus are shifted linearly with the applied source-drain voltage. Based on this prediction we discuss a method proposed for measuring the energy spacings of the sublevels of the constriction. Under the assumption that the transmission of an electron depends only on the difference between the energy of the electron incident on the constriction and the bottom of the electrostatic confining potential, a simple analytical form is derived for the nonlinear differential conductance of the constriction. This form complements our exact calculational results and shows that at zero temperature the differential conductance at a given finite V_{sd} and a given Fermi energy E_F is a weighted average of two zero-V_{sd} conductances at Fermi energies of $E_F+(1-\alpha)eV_{sd}$ and $E_F-\alpha eV_{sd}$, where α describes the fraction of the source-drain voltage that drops on the connection between the constriction and the drain reservoir.

I. INTRODUCTION

Recent advances in nanostructure technology[1] have made it possible to define quasi-one-dimensional (Q1D) constrictions, with lateral dimensions on the order of 100 nm, in a two-dimensional electron gas (2DEG) formed at a semiconductor heterostructure. In such a tiny structure, the electron transport becomes ballistic and the motion of electrons is governed by quantum mechanics rather than classical mechanics, revealing a few very interesting features in electron transport.[2] In particular, it has been well known that in the linear-response regime of transport the conductance of the Q1D constrictions is sharply quantized in units of $2e^2/h$ at low temperatures.[3,4] This fascinating phenomenon has now been well understood, thanks to a number of theoretical calculations including those using adiabatic approximation and/or the Landauer formula, and those based on exact quantum-mechanical formulations.[5–12]

Recently, a few experiments have been devoted to the study of the nonlinear behavior of the conductance of Q1D systems under high dc source-drain voltage V_{sd}. The first experiment was reported by Kouwenhoven *et al.*[13] for a Q1D device defined by quantum point contacts. They found that breakdown of the conductance quantization occurs when eV_{sd} is equal to the sublevel separation at the Fermi energy of the device, as manifested by either an increase or a decrease in the differential conductance G from the quantized values of the multiples of $2e^2/h$. In the measurements on a split gate device by Patel *et al.*,[14,15] additional quantized conductance plateaus (called half plateaus) at values intermediate between the multiples of $2e^2/h$ were observed when $G > 2e^2/h$. For $G < 2e^2/h$, Patel *et al.* claim that there is no half plateau, but rather anomalous structure at conductances of $0.2(2e^2/h)$ and $0.8(2e^2/h)$.[14,15] Theoretical calculations on the conductance of Q1D constrictions were also carried out for the nonlinear regime of transport. In an adiabatic calculation[16] Glazman and Khaetskii obtained the half conductance plateaus for a constriction whose width varies very slowly. The half plateau structure was also obtained in a very recent calculation by Martin-Moreno *et al.*,[17] who modeled Q1D constriction by a saddle-point potential. However, the half plateaus did not appear in the quantum-mechanical calculations of Castaño and Kirczenow[18] for a constriction defined by abrupt changes in geometry. Furthermore, there was no indication of the existence of the half plateaus in even earlier calculations by Lent, Sivaprakasam, and Kirkner[19] for a wide-narrow-wide quantum device which is actually very similar to the model structure of Castaño and Kirczenow. Do these contradictory predictions mean that the half plateaus are the special property of transport that can only be obtained in adiabatic model calculations? It is the purpose of this work to address this question. We will demonstrate that this nonlinear property of ballistic transport can also appear in the calculated conductance for the constrictions defined by abrupt changes in geometry.

II. THEORY

We base our work on quantum-mechanical calculations of the differential conductance of a narrow constriction as shown schematically in Fig. 1. The narrow constriction is connected to two 2DEG reservoirs that are assumed to remain in the local equilibrium with electrochemical potentials μ_1 and μ_2, respectively. We consider a finite temperature in general and assume that phase-breaking processes occur only deep inside the two reservoirs. The difference between the electrochemical potentials μ_1 and μ_2 is related to the applied source-drain voltage V_{sd} according to $eV_{sd}=\mu_1-\mu_2$. The electrostatic potential U in the constriction should in general depend both on position and on the source-drain voltage V_{sd} at a given temperature. In principle, the profile of the electrostatic potential U can be calculated from the confinement potential and the charge density in the constriction. The charge density is determined by the solutions of the Schrödinger's equation of the system, which in turn is related to the electrostatic potential U. In an exact procedure, one would have to use an iterative method to find the self-consistent electrostatic potential U for the constriction subject to the given source-drain voltage V_{sd} and temperature. So far, no such attempts have been reported and all theoretical calculations have been based on assumptions about how the source-drain voltage V_{sd} is dropped along the constriction. Glazman and Khaetskii assumed that half of the source-drain voltage V_{sd} is dropped between the source reservoir and the narrowest part of the constriction, while Castaño and Kirczenow, and Lent, Sivaprakasam, and Kirkner assumed that the voltage V_{sd} is dropped linearly along the constriction. In the present calculations we assume a steplike voltage drop along the Q1D constriction, i.e., the voltage drops occur only at the two ends of the constriction. We believe that this assumption is appropriate for our model constriction, because in the ballistic transport there are no electron backscatterings in our model constriction except at its entry and exit. This assumption is also in accordance with a recent lowest-order calculation by Bandyopadhyay *et al.*[20] for a rectangular constriction with repulsive impurities, in which it was shown that the electrostatic potential in the constriction remains rather flat along the transport direction and the potential drop occurs mainly at the two ends of the constriction. Under this assumption we may write the electrostatic potential U, together with the electrochemical potentials μ_1 and μ_2 in the two reservoirs, as

$$U=U_c(y)+\alpha eV_{sd} , \tag{1}$$

$$\mu_1=\mu_F+eV_{sd}, \tag{2}$$

$$\mu_2=\mu_F , \tag{3}$$

where $U_c(y)$ is the confinement potential defining the constriction at $V_{sd}=0$, α is a parameter between 0 and 1 describing the fraction of the voltage V_{sd} that drops on the connection between the constriction and the drain reservoir, and μ_F is the electrochemical potential of the reservoirs at zero source-drain voltage. In this work, the constriction under our consideration is symmetric. We will thus assume that $\alpha=\frac{1}{2}$, i.e., the electrostatic potential drops equally at the connections between the constriction and the source reservoir and between the constriction and the drain reservoir.

Assuming the Fermi-Dirac distribution for the electrons inside the two reservoirs, we can simply write the current through the constriction as

$$I(\mu_F,V_{sd},T)=\int_0^\infty J(\varepsilon,V_{sd})\{f(\varepsilon-(\mu_F+eV_{sd}),T) -f(\varepsilon-\mu_F,T)\}d\varepsilon , \tag{4}$$

where $J(\varepsilon,V_{sd})d\varepsilon$ is the total current summed over all possible incident waves at energy range between ε and $\varepsilon+d\varepsilon$ from the left reservoir, f is the Fermi-Dirac function, and T is the temperature at the two reservoirs. The differential conductance of the constriction is then given by

$$\begin{aligned} G(\mu_F,V_{sd},T)&\equiv\frac{\partial I(\mu_F,V_{sd},T)}{\partial V_{sd}} \\ &=\int_0^\infty J(\varepsilon,V_{sd})\frac{\partial f(\varepsilon-(\mu_F+eV_{sd}),T)}{\partial V_{sd}}d\varepsilon \\ &\quad+\int_0^\infty \frac{\partial J(\varepsilon,V_{sd})}{\partial V_{sd}}\{f(\varepsilon-(\mu_F+eV_{sd}),T) -f(\varepsilon-\mu_F,T)\}d\varepsilon . \end{aligned} \tag{5}$$

In the linear-response regime of transport, where it is assumed that $V_{sd}\to 0$, the second term in Eq. (5) can be dropped. The conductance in the linear-response regime of transport is then

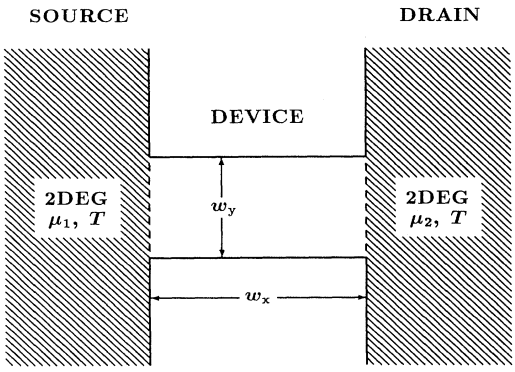

FIG. 1. Schematic representation of a mesoscopic device defined by a finite quantum channel of length w_x and width w_y. The channel is connected with two semi-infinite 2DEG's, which are assumed to remain in the local equilibrium with electrochemical potentials μ_1 and μ_2, respectively, and act as source and drain when a potential difference is applied. The device is assumed to be operated at a finite temperature T. Phase-breaking processes are assumed to occur only in the two 2DEG's.

$$G_0(\mu_F,T)\equiv G(\mu_F,V_{sd},T)|_{V_{sd}\to 0}$$
$$=-e\int_0^\infty J_0(\varepsilon)\frac{\partial f(\varepsilon-\mu_F,T)}{\partial\varepsilon}d\varepsilon\ , \tag{6}$$

where

$$J_0(\varepsilon)\equiv J(\varepsilon,V_{sd}\to 0) \tag{7}$$

is, in fact, the total current per energy through the constriction defined by $U_c(y)$ at energy ε. At zero temperature, the conductance $G_0(\mu_F,T)$ is simply reduced to

$$G_0(\mu_F)\equiv G_0(\mu_F,T)|_{T\to 0}=eJ_0(\mu_F)\ , \tag{8}$$

and μ_F is now the Fermi energy of the two reservoirs.

In fact, the assumption of Eq. (1) means that by applying a finite source-drain voltage V_{sd} to a constriction, the confinement potential of the constriction will be shifted upward by αeV_{sd}. Therefore, in many cases, it should be a good approximation to assume that $J(\varepsilon,V_{sd})=J_0(\varepsilon-\alpha eV_{sd})$ (see Sec. III for the calculations). Inserting this assumption to Eqs. (4) and (5), one may have

$$I(\mu_F,V_{sd},T)=\int_0^\infty J_0(\varepsilon)\{f(\varepsilon-[\mu_F+(1-\alpha)eV_{sd}],T)-f(\varepsilon-(\mu_F-\alpha eV_{sd}),T)\}d\varepsilon \tag{9}$$

and

$$G(\mu_F,V_{sd},T)=\int_0^\infty J_0(\varepsilon)\left\{\frac{\partial f(\varepsilon-[\mu_F+(1-\alpha)eV_{sd}],T)}{\partial V_{sd}}-\frac{\partial f(\varepsilon-(\mu_F-\alpha eV_{sd}),V)}{\partial V_{sd}}\right\}d\varepsilon\ . \tag{10}$$

At zero temperature, the nonlinear conductance represented by the above equation can be directly calculated from the conductances obtained in the linear-response regime of transport

$$G(\mu_F,V_{sd})\equiv G(\mu_F,V_{sd},T)|_{T\to 0}$$
$$=(1-\alpha)G_0(\mu_F+(1-\alpha)eV_{sd})$$
$$+\alpha\vartheta(\mu_F-\alpha eV_{sd})G_0(\mu_F-\alpha eV_{sd})\ , \tag{11}$$

where $\vartheta(x)$ is the unit step function, i.e., $\vartheta(x)=1$ for $x>0$ and $\vartheta(x)=0$ for $x<0$. Equation (11) simply indicates that at zero temperature, the differential conductance at finite V_{sd} is the weighted average of two zero-V_{sd} conductances at Fermi energies of $\mu_F+(1-\alpha)eV_{sd}$ and $\mu_F-\alpha eV_{sd}$. In the adiabatic approximation, the zero-V_{sd} conductance at zero temperature can be written as[3,14,15]

$$G_0(E_F)=\frac{2e^2}{h}N(E_F)\ , \tag{12}$$

where $N(E_F)$ is the number of transverse modes of the Q1D constriction with energies below Fermi energy E_F. Inserting this into Eq. (11), the differential conductance at zero temperature is then simplified to, after replacing μ_F by E_F for clarity,

$$G(E_F,V_{sd})=\frac{2e^2}{h}\{(1-\alpha)N(E_F+(1-\alpha)eV_{sd})$$
$$+\alpha N(E_F-\alpha eV_{sd})\}\ . \tag{13}$$

For $\alpha=0.5$, Eq. (13) predicts that in addition to the zero-V_{sd} quantized conductance plateaus at the values of the multiples of $2e^2/h$, half plateaus will appear exactly at the values of the half-integer multiples of $2e^2/h$.

In order to obtain the current through the constriction from Eq. (4) and the differential conductance of the constriction from Eq. (5), we have to carry out the exact calculations for the quantity $J(\varepsilon,V_{sd})$, i.e., the total current per energy summed over all possible incident waves of electrons at energy ε from the left reservoir. Such calculations are, however, quite elementary.[9,21,22] Here only a brief outline of the formalism is presented.

Consider an electron with wave vector $\mathbf{k}=(k_x,k_y)$ and energy ε, where $\varepsilon=\hbar^2(k_x^2+k_y^2)/(2m^*)$ while m^* is the effective mass of the electron, incident from the left 2DEG reservoir on the constriction with the effective electrostatic potential defined by Eq. (1) and emitted to the right. The wave function of the electron on the left and right 2DEG reservoirs can be written, respectively, as

$$\Psi^L(x,y)=e^{ik_x(x-x_0^L)}\phi_{k_y}^{2D}(y)$$
$$+\int_{-\infty}^{\infty}dk_y'\,A_{k_y'}^L e^{-ik_x'(x-x_0^L)}\phi_{k_y'}^{2D}(y)\ , \tag{14}$$

$$\Psi^R(x,y)=\int_{-\infty}^{\infty}dk_y'\,A_{k_y'}^R e^{ik_x'(x-x_0^R)}\phi_{k_y'}^{2D}(y)\ , \tag{15}$$

where $\phi_{k_y}^{2D}(y)=(2\pi)^{-1/2}\exp(ik_y y)$, $k_x'=[2m^*\varepsilon/\hbar^2-(k_y')^2]^{1/2}$, and x_0^L and x_0^R stand for the x coordinates of the left and right ends of constriction, respectively. Here the integral is taken over all transverse components k_y' and thus k_x' can be either real or imaginary, i.e., evanescent waves are included. Here we note that in the case that k_x' is imaginary, the convention $(-1)^{1/2}=i$ is used. The wave function of the electron in the constriction can be written as

$$\Psi^C(x,y)=\sum_n[b_n e^{ik_n(x-x_0^L)}+c_n e^{-ik_n(x-x_0^L)}]\phi_n^C(y)\ , \tag{16}$$

where $\phi_n^C(y)$ are a set of transverse eigenstates in the constriction with eigenvalues E_n, satisfying the one-dimensional Schrödinger equation

$$\left[-\frac{\hbar^2}{2m^*}\frac{d^2}{dy^2}+U_c(y)\right]\phi_n^C(y)=E_n\phi_n^C(y)\ . \tag{17}$$

The quantities k_n in Eq. (16) are given by

$$k_n = \left[\frac{2m^*(\varepsilon - \alpha e V_{sd} - E_n)}{\hbar^2} \right]^{1/2} . \quad (18)$$

Again, the summation in Eq. (16) is taken over all n values in order to include all evanescent and current transporting waves.

As usual, $\Psi^C(x,y)$ needs to be matched to $\Psi^L(x,y)$ at $x = x_0^L$ and to $\Psi^R(x,y)$ at $x = x_0^R$ with the requirement that amplitudes and derivatives with respect to x are equal. After eliminating $A_{k_y'}^L$ and $A_{k_y'}^R$ from the resulting equations of the matching, we can obtain a set of linear equations from which all expansion coefficients b_n and c_n in Eq. (16) can be determined. The electric current carried through the constriction by the wave function of the electron characterized by its wave vector $\mathbf{k} = (k_x, k_y)$ in the left reservoir can be expressed in terms of the expansion coefficients of the wave function in the constriction,[21]

$$J_{\mathbf{k}}(\varepsilon, \vartheta, V_{sd}) = -\frac{e\hbar}{m^*} \left[\sum_n^{(R)} k_n (b_n b_n^* - c_n c_n^*) + \sum_n^{(I)} k_n (b_n c_n^* - c_n b_n^*) \right] , \quad (19)$$

where ϑ specifies the incident direction of the electron wave in the left reservoir and is defined as $\sin(\vartheta) = k_y / |k_x^2 + k_y^2|^{1/2}$, $\varepsilon = \hbar^2(k_x^2 + k_y^2)/2m^*$ is the energy of the incident electron, (R) $[(I)]$ indicates that the sum is taken over those values of n for which k_n is real (imaginary). By integrating over all possible incident waves $\mathbf{k}$ on the constriction in the energy range between ε and $\varepsilon + d\varepsilon$ from the left reservoir, we obtain after dividing by $d\varepsilon$

$$J(\varepsilon, V_{sd}) = \frac{4\pi m^*}{h^2} \int_{-\pi/2}^{\pi/2} d\vartheta \, J(\varepsilon, \vartheta, V_{sd}) = -\frac{2e}{h} \int_{-\pi/2}^{\pi/2} d\vartheta \left[\sum_n^{(R)} k_n (b_n b_n^* - c_n c_n^*) + \sum_n^{(I)} k_n (b_n c_n^* - c_n b_n^*) \right] . \quad (20)$$

Here we wish to clarify that in the integrand of Eq. (20), only the expansion coefficients b_n and c_n are functions of ϑ, i.e., the direction of the incident wave of electrons on the constriction from the left reservoir. We note also that even the formulation presented above for the quantity $J(\varepsilon, V_{sd})$ is exact; the expansion coefficients b_n and c_n, however, have to be calculated numerically by truncating n at a high transverse level M. In the present calculations we allow M to be as large as is necessary to obtain a desired convergence in the differential conductance, and we do not need to go beyond $M = 10$.

III. RESULTS AND DISCUSSION

Figures 2–5 summarize some of our calculated results for the Q1D constriction of Fig. 1 with $w_x = 200$ nm and $w_y = 100$ nm. We have assumed a square-well potential for the Q1D constriction with its bottom at $U_0 = 1.0$ meV when $V_{sd} = 0$ and an electron effective mass $m^* = 0.067 m_e$ which is appropriate to the $Al_xGa_{1-x}As/GaAs$ interface.

In Fig. 2 we have plotted, as solid lines, the differential conductance $G(\mu_F, V_{sd}, T)$ calculated from Eq. (5) at temperature $T = 10$ mK versus the electrochemical potential μ_F at various source-drain voltages V_{sd}. The lowest trace in the figure is for $V_{sd} = 4.0$ mV, and the successive traces, calculated as V_{sd} was decreased in steps of 0.5 mV, have been offset in the vertical direction for clarity. Thus the highest trace is for $V_{sd} = 0$ and has been vertically offset by $8.0(2e^2/h)$. It can be seen that at $V_{sd} = 0$ the differential conductance shows the quantum feature, i.e., that the differential conductance is quantized in units of $2e^2/h$, and the modulations superimposed on the conductance plateaus. These modulations appear to be due to transmission resonances that are formed as we have defined our constriction by the abrupt changes of geometry. Because of the existence of the modulation structure we may identify the edge of each conductance plateau by a relatively sharp resonant peak. In models that consider an adiabatic change in geometry, this modulation structure may not appear. In these cases, one may need to calculate $\partial G / \partial \mu_F$, the derivative of the

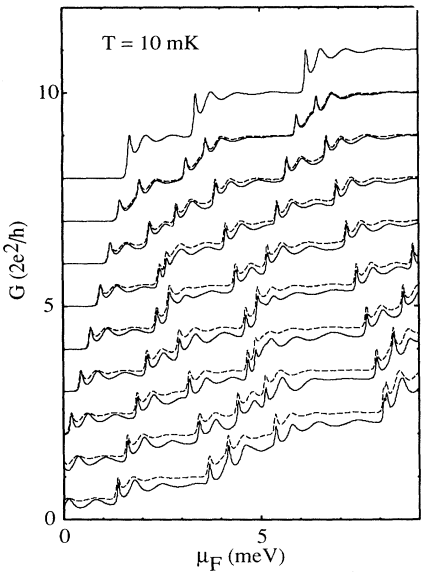

FIG. 2. The calculated differential conductance G vs electrochemical potential μ_F, at $T = 10$ mK and at various source-drain voltages, for the quantum device as shown in Fig. 1 with $w_x = 200$ nm, $w_y = 100$ nm. The quantum channel is defined by a square-well potential with its bottom at $U_0 = 1.0$ meV when $V_{sd} = 0$. The lowest trace in the figure is for $V_{sd} = 4.0$ mV, and the successive traces, calculated as V_{sd} was decreased in steps of 0.5 mV, have been vertically offset from each other by a quanta $2e^2/h$. The highest trace is thus for $V_{sd} = 0$ and has been vertically offset by $8.0(2e^2/h)$. The solid curves show the exact calculations from Eq. (5), while the dashed curves are the approximate results from Eq. (10).

differential conductance G with respect to the electrochemical potential μ_F, and to identify the edges of the conductance plateaus by the peaks in the calculated traces of $\partial G/\partial\mu_F$.[23] It is shown in Fig. 2 that as the source-drain voltage is increased, a new plateau structure develops at conductance values somewhere intermediate between the zero-voltage quantization values. This indicates an additional quantization in the differential conductance at finite source-drain voltages.

The development of the new plateau structure may be traced out even more easily if we follow the evolution of the sharp resonant peaks at the edges of the conductance plateaus with increasing V_{sd}. In general, at a given finite source-drain voltage the zero-V_{sd} resonant peak at the edge of each conductance plateau is split into two peaks. In this work, the two voltage-induced peaks are labeled n^- and n^+ according to whether they move to lower or higher electrochemical potential, respectively, where n indicates the two peaks are formed from the sharp resonant peaks at the edge of the nth zero-V_{sd} conductance plateau. We have found that the shifts in the electrochemical potentials of the two voltage-induced peaks are linearly dependent on the source-drain voltage, as indicated by Eq. (11) at very low temperature. This linearity in the evolution of the voltage-induced peaks may be seen even more clearly in Fig. 3, where the electrochemical potentials at which the sharp resonant peaks at the edges of conductance plateaus appear are plotted versus V_{sd}.

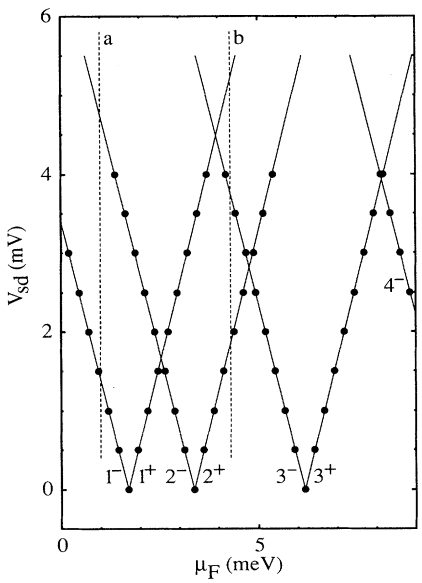

FIG. 3. The variation of the electrochemical potential positions of the sharp resonant peaks at the edges of a few of the lowest conductance plateaus as a function of the applied source-drain voltage at $T=10$ mK. The solid circles in this figure correspond to the results extracted from the traces presented in Fig. 2. The dashed vertical lines, labeled a and b, are drawn, as examples, for determination of the energy spacings of the sublevels of the quantum constriction from the figure (see the text).

We wish to note here that for convenience we have set, in Fig. 3, the source-drain voltage to be increased when going from the bottom to the top of the figure, as opposed to that in Fig. 2. The solid circles in Fig. 3 correspond to the results extracted from the exact calculations presented in Fig. 2. By denoting the electrochemical-potential positions of the n^- and n^+ peaks by $E(n^-)$ and $E(n^+)$, respectively, we may define the electrochemical-potential-shift coefficients of the two peaks by $\eta(n^-)\equiv dE(n^-)/d(eV_{sd})$ and $\eta(n^+)\equiv dE(n^+)/d(eV_{sd})$. For the device structure we have studied with $\alpha=\frac{1}{2}$ [see Eq. (1)], it is found that $\eta(n^-)=-0.5$ and $\eta(n^+)=0.5$. The electrochemical-potential-splitting coefficient $\eta(n)$ of the n^- and n^+ peaks is thus given by $\eta(n)\equiv\eta(n^+)-\eta(n^-)=1$. The voltage-induced n^- and n^+ peaks have, in general, different heights. As the source-drain voltage is incremented from zero, the n^- peak is found to be lowered approximately by a half of a quanta $2e^2/h$ from the height of the zero-voltage peak at the edge of the nth conductance plateau, while the n^+ peak is found to remain roughly at the height of the zero-voltage peak. Thus, at a small but finite source-drain voltage, in addition to the appearance of new conductance plateaus at values approximately midway between the multiples of $2e^2/h$, all the conductance plateaus observed at $V_{sd}=0$ are preserved.

It is clear that at certain source-drain voltages, the $(n+m)^-$ and n^+ peaks will coincide, where $m=1,2,3,\ldots$, and thus conductance plateaus can be destroyed. It is easy to deduce that such coincidences and destructions will occur when the source-drain voltage V_{sd} satisfies that $eV_{sd}=E_{n+m}-E_n$, where E_n is the nth sublevel energy of the Q1D constriction at $V_{sd}=0$. In Fig. 4 we have plotted, as solid lines, the differential conductance versus the electrochemical potential μ_F for four different source-drain voltages V_{sd} selected such that (a) $eV_{sd}=E_2-E_1$, (b) $eV_{sd}=E_3-E_2$, (c) $eV_{sd}=E_4-E_3$, and (d) $eV_{sd}=E_3-E_1$. Here we see that the first, second, and third integer conductance plateaus, which we saw at $V_{sd}=0$, do not appear in the calculated traces of the differential conductance at $V_{sd}=(E_2-E_1)/e$ [curve (a)], $V_{sd}=(E_3-E_2)/e$ [curve (b)], and $V_{sd}=(E_4-E_3)/e$ [curve (c)], respectively. For example, at $V_{sd}=(E_2-E_1)/e$ [see curve (a)], the step value of the first conductance plateau is close to a half of quanta $2e^2/h$ while the step value of the second plateau is close to three-halves of quanta $2e^2/h$. Both are one-half of quanta $2e^2/h$ away from the first integer quantization conductance value at $V_{sd}=0$. Curve (d) shows that at $eV_{sd}=E_3-E_1$, all integer plateaus remain in the calculated differential conductance, but the second half-integer plateau at a conductance value close to three-halves of quanta $2e^2/h$ is destroyed.

In Figs. 2 and 4 we also show the differential conductance curves (dashed lines) at the various source-drain voltages, calculated from Eq. (10) where the assumption $J(\varepsilon,V_{sd})=J_0(\varepsilon-\alpha eV_{sd})$ was made. We can see that the calculated differential conductance under this assumption retains all features, e.g., resonant peaks and additional half-integer conductance plateaus, that were obtained in

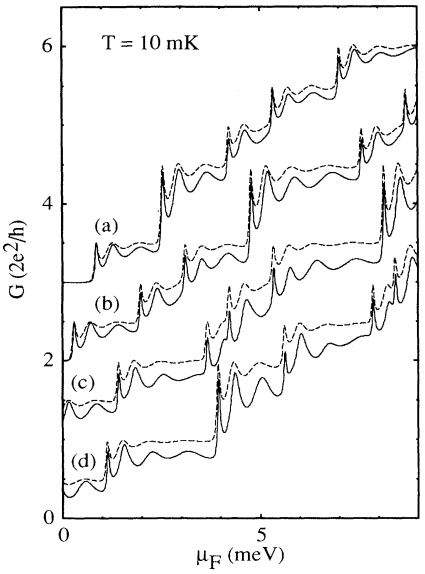

FIG. 4. The calculated differential conductance G vs electrochemical potential μ_F, at $T=10$ mK and at four selected source-drain voltages, for the quantum device as shown in Fig. 1 with $w_x=200$ nm, $w_y=100$ nm. The four selected source-drain voltages are (a) $V_{sd}=(E_2-E_1)/e$, (b) $V_{sd}=(E_3-E_2)/e$, (c) $V_{sd}=(E_4-E_3)/e$, and (d) $V_{sd}=(E_3-E_1)/e$, where E_n is the nth sublevel energy of the quantum channel at $V_{sd}=0$. The quantum channel is defined by a square-well potential with its bottom at $U_0=1.0$ meV when $V_{sd}=0$. The traces have been vertically offset from each other by a quanta $2e^2/h$ from bottom (d) to top (a). The solid curves show the exact calculations from Eq. (5), while the dashed curves are the approximate results from Eq. (10).

the exact calculations from Eq. (5). However, the differential conductance is found to be quantized in conductance values closer to integer and half-integer multiples of $2e^2/h$ under this assumption than in the exact calculations. It can be seen that the deviation of the calculations under this assumption from the exact results is larger at higher source-drain voltages. In fact, this assumption is more proper for adiabatic constrictions for which theoretical calculations predict rather perfect plateaus in conductance, but not resonant structure on the plateaus. Since adiabatic constrictions are more realistic for real device structures, Eqs. (10), (11), and (13) may directly be used to explain experimental measurements.

It can also be seen in Figs. 2 and 3 that as the source-drain voltage is further increased from a value given by $V_{sd}=(E_{n+m}-E_n)/e$, the coincident conductance peak formed from the $(n+m)^-$ and n^+ peaks will split again into two peaks. We find that the two peaks have the same electrochemical-potential-shift coefficients with respect to V_{sd} as the $(n+m)^-$ and n^+ peaks before their coincidence into a single peak. Thus the peak moving to a lower electrochemical potential is still labeled $(n+m)^-$ and the other one which moves to higher electrochemical potential is labeled n^+ (see Fig. 3). In general, as V_{sd} sweeps over the source-drain voltage given by $V_{sd}=(E_{n+m}-E_n)/e$, the conductance plateau with its edge marked by the $n^+[(n+m)^-]$ peak will raise (lower) its step value approximately by a half of quanta $2e^2/h$. Therefore, the differential conductance is again quantized approximately in all integer and all half-integer multiples of $2e^2/h$. This nonlinear behavior in the differential conductance will be preserved, so long as V_{sd} is lower than the next critical source-drain voltage at which another pair of peaks at edges of conductance plateaus become coincident.

In a partial summary, we have predicted that with increasing V_{sd} from the linear-response regime of transport, the half-integer conductance plateaus are formed from the integer plateaus. We have shown that both the half-integer and the integer plateaus will be preserved until V_{sd} reaches the first critical source-drain voltage given by $V_{sd}=(E_2-E_1)/e$. When $V_{sd}=(E_2-E_1)/e$, the first integer plateau will be destroyed. As V_{sd} is further increased, this integer plateau will reappear. Such destructions and reappearances of the integer plateaus will occur in general whenever the source-drain voltage sweeps over the critical values of $V_{sd}=(E_{n+1}-E_n)/e$. We have found that the half-integer plateaus will also be destroyed when $V_{sd}=(E_{n+2}-E_n)/e$. For example, the destruction of the second half-integer plateau at a conductance value close to $1.5(2e^2/h)$ will occur when $V_{sd}=(E_3-E_1)/e$. We can argue that ideally we should see the destructions and the reappearances of integer (half-integer) plateaus as V_{sd} sweeps over all the voltages given by $V_{sd}=(E_{n+m}-E_n)/e$ with m being positive odd (even) integers. We have shown that the first half-integer plateau will be preserved in the calculated differential conductances for all finite source-drain voltages. In fact, it can be deduced from Eq. (11) that for $V_{sd}>(E_n-E_1)/e$ all first n plateaus, counting in both half-integer and integer plateaus, should remain in the differential conductances at low temperature. However, these conductance plateaus are not always seen in the calculated differential conductances (see Figs. 2 and 4). For a given source-drain voltage, the initial conductance of a device, defined as the conductance at the electrochemical potential in the drain reservoir $\mu_F=0$, may be well larger than the conductances of several lowest plateaus. All the plateaus with conductances lower than the initial conductance of the device cannot be seen. We may generate these lowest conductance plateaus by decreasing the width of the Q1D channel, since the initial conductance of the channel is lowered as its width is decreased.

From the traces of differential conductances, it is possible to determine the energy spacings of sublevels for a given Q1D constriction. This can be done simply with use of the linearity feature in the development of the resonant peaks at the edges of conductance plateaus with an applied source-drain voltage, as we depicted in Fig. 3. Let us draw a vertical line in Fig. 3 through the electrochemical potential μ_F. This line will intersect those lines labeled n^+ and/or n^- in the figure. It should be easy to work out the source-drain voltages at which these intersections occur. These source-drain voltages may be labeled V_{n+} or V_{n-} according to the index of those lines that the vertical line intersects. Let us further denote the

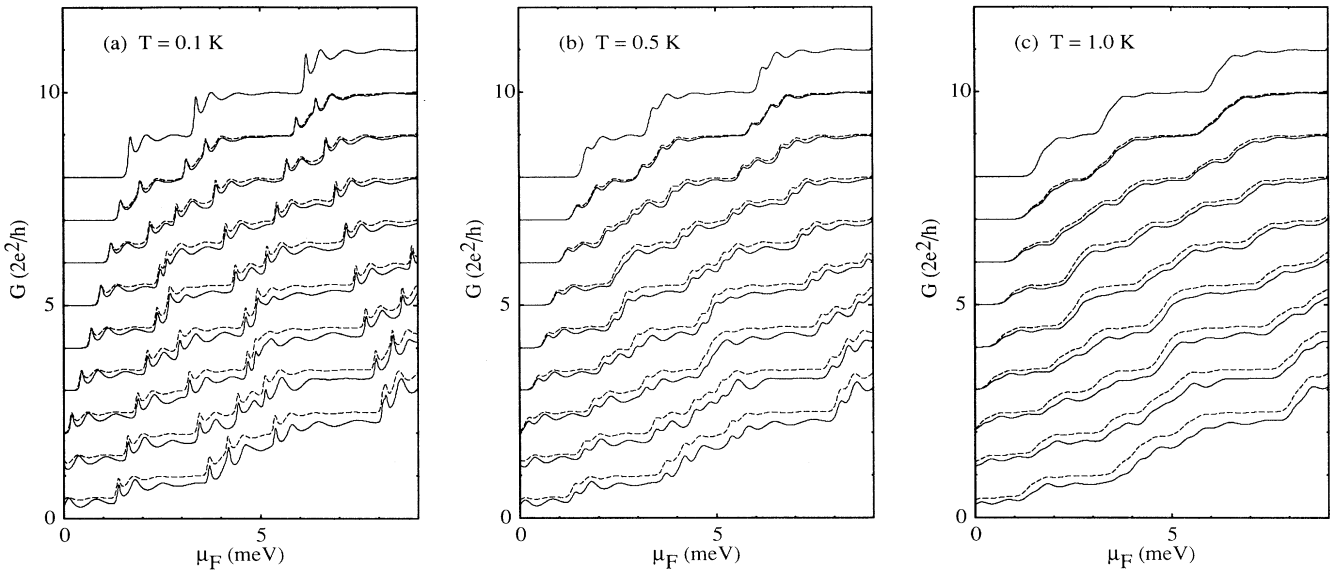

FIG. 5. The calculated differential conductance G vs electrochemical potential μ_F, at various source-drain voltages, for the quantum device as shown in Fig. 1 with $w_x=200$ nm, $w_y=100$ nm at (a) $T=0.1$ K, (b) $T=0.5$ K, and (c) $T=1.0$ K. The quantum channel is defined by a square-well potential with its bottom at $U_0=1.0$ meV when $V_{sd}=0$. The lowest trace in each figure is for $V_{sd}=4.0$ mV, and the successive traces, calculated as V_{sd} was decreased in steps of 0.5 mV, have been vertically offset from each other by a quanta $2e^2/h$. The highest trace in each figure is thus for $V_{sd}=0$ and has been vertically offset by $8.0(2e^2/h)$. The solid curves show the exact calculations from Eq. (5), while the dashed curves are the approximate results from Eq. (10).

electrochemical potentials, at which the sharp resonant peaks at the edges of the zero-voltage conductance plateaus are seen, by $E(n)$, where $n=1,2,3,\ldots$. The energy spacings of the sublevels can then be calculated from V_{n+} and/or V_{n-} as follows. For the electrochemical potential μ_F to be somewhere below $E(1)$, we have

$$E_n-E_1=\tfrac{1}{2}e(V_{n-}-V_{1-}),\quad n>1\ , \tag{21}$$

where E_n, $n=1,2,3,\ldots$, are sublevel energies of the constriction. For μ_F to be somewhere between $E(n)$ and $E(n+1)$, we have

$$E_{n+m}-E_n=\tfrac{1}{2}e(V_{n+}+V_{(n+m)-}),\quad m\geq 1\ , \tag{22}$$

$$E_n-E_{n-m}=\tfrac{1}{2}e(V_{(n-m)+}-V_{n+}),\quad m\geq 1\ . \tag{23}$$

For example, the vertical line labeled a in Fig. 3, through $\mu_F=1.0$ meV, is seen to intersect evolution lines 1^- and 2^-, yielding $V_{1-}=1.39$ mV and $V_{2-}=4.75$ mV. Using Eq. (21) with $n=2$, we obtain the energy spacing between the first and second sublevels of the constriction, $E_2-E_1=1.68$ meV [compared with the exact value of the energy spacing, $(\hbar^2/2m^*)(\pi/w_y)^2(2^2-1)\approx 1.6837$ meV]. The vertical line b, through $\mu_F=4.3$ meV, is seen to intersect evolution lines 2^+, 3^-, and 1^+ in Fig. 3, resulting in $V_{2+}=1.86$ mV, $V_{3-}=3.76$ mV, and $V_{1+}=5.22$ mV. Using Eqs. (22) and (23) with $n=2$ and $m=1$, we obtain $E_3-E_2=2.81$ meV [compared with the exact value of the energy spacing, $(\hbar^2/2m^*)(\pi/w_y)^2(3^2-2^2)\approx 2.8062$ meV] and again $E_2-E_1=1.68$ meV, respectively.

All above results are obtained at very low temperature ($T=10$ mK) and under the assumption that the Q1D constriction has a square-well confining potential with hard-wall boundaries. The calculated differential conductances of the Q1D constriction at three different temperatures are shown in Fig. 5. It can be seen that for the device structure we have assumed the integer and half-integer conductance plateaus and the resonant structure superimposed on them are well preserved at $T=100$ mK. The resonant structure becomes weak at $T=500$ mK and is well smoothed out at $T=1$ K, whereas the integer and the half-integer plateaus can still be clearly identified at these temperatures. Using a square-well Q1D confining potential with hard-wall boundaries, we obtain a set of unequally energy-spaced sublevels. Thus the destructions and reappearances of different integer conductance plateaus are seen to occur, in general, at different source-drain voltages. Different half-integer plateaus will be destroyed and reappear at different source-drain voltages too. If one assumes a parabolic confining potential in the Q1D constriction, one should see the destructions and reappearances of integer plateaus at the same source-drain voltages. The destructions and reappearances of half-integer plateaus will also occur at the same times in this case.

IV. CONCLUSIONS

In conclusion, we have investigated the effect of applying a finite source-drain voltage across a uniform Q1D ballistic constriction, based on quantum-mechanical model calculations. In accordance with the fact that no

backscattering could occur inside the considered Q1D constriction, the sharp drops of electrostatic potential at the ends of the constriction have been assumed. We have shown that the half-integer conductance plateaus are formed at finite source-drain voltages. For the constriction we have considered, the resonant structure is seen to be superimposed on the half-integer and the integer plateaus at very low temperatures. Thus the edges of conductance plateaus can be identified by these sharp resonant peaks. We have found that the edges of the conductance plateaus are shifted linearly with the applied source-drain voltage. This theoretical result could be used to determine the sublevel energy spacings for a Q1D constriction from experimental measurements. Under the assumption that the transmission of an electron depends only on the difference between the energy of the electron incident on the constriction and the bottom of the electrostatic potential of the confinement, a simple analytical form has been derived for the nonlinear differential conductance of the constriction, which highlights our exact calculational results and states that at zero temperature the differential conductance at a given finite V_{sd} and a given Fermi energy E_F is a weighted average of two zero-V_{sd} conductances at Fermi energies of $E_F+(1-\alpha)eV_{sd}$ and $E_F-\alpha eV_{sd}$, where α describes the fraction of the source-drain voltage that drops on the connection between the constriction and the drain reservoir. We have predicted that both the integer and voltage-induced half-integer plateaus can be destroyed and reappear as the source-drain voltage is increased. However, it has been predicted that the destruction should not occur on the lowest half-integer plateau.

ACKNOWLEDGMENTS

The author is grateful to K.-F. Berggren at Linköping University for many stimulating discussions. The author wishes to thank P. Omling and L. Samuelson at University of Lund for encouragement, support, and helpful conversations. The calculations have been done in part on the computing facilities of the Solid State Theory Group, Department of Theoretical Physics, University of Lund. This work, which is performed within the nm–consortium in Lund, has been supported by the Swedish Natural Science Research Council and the Swedish National Board for Technical Developments.

*Address to which correspondence should be diverted.

[1]See, e.g., M. L. Roukes *et al.*, in *Science and Engineering of 1- and 0-Dimensional Semiconductors,* edited by S. P. Beaumont and C. M. Sotomayor-Torres (Plenum, New York, 1989), for a survey of microfabrication techniques of nanostructures.

[2]C. W. Beenakker and H. van Houten, in *Solid State Physics: Advances in Research and Applications,* edited by H. Ehrenreich and D. Turnbull (Academic, New York, 1991), Vol. 44, p. 1.

[3]B. J. van Wees, H. van Houtenk, C. W. J. Beenakker, J. G. Williamson, L. P. Kouwenhoven, D. van der Marel, and C. T. Foxon, Phys. Rev. Lett. **60**, 848 (1988).

[4]D. A. Wharam, T. J. Thornton, R. Newbury, M. Pepper, and H. Ahmed, J. Phys. C **21**, L209 (1988).

[5]R. Landauer, Z. Phys. B **68**, 217 (1987).

[6]M. Büttiker, Y. Imry, R. Landauer, and S. Pinhas, Phys. Rev. B **31**, 6207 (1985).

[7]A. Szafer and A. D. Stone, Phys. Rev. Lett. **62**, 300 (1989).

[8]E. G. Haanappel and D. van des Marel, Phys. Rev. B **39**, 5484 (1989).

[9]G. Kirczenow, Solid State Commun. **68**, 715 (1988); J. Phys. Condens. Matter **1**, 305 (1989); Phys. Rev. B **39**, 10 452 (1989).

[10]E. Tekman and S. Ciraci, Phys. Rev. B **39**, 8772 (1989); **40**, 8559 (1989).

[11]L. Escapa and N. Garcia, J. Phys. Condens. Matter **1**, 2125 (1989).

[12]M. Yosefin and M. Kaveh, Phys. Rev. Lett. **64**, 2819 (1990).

[13]L. P. Kouwenhoven, B. J. van Wees, C. J. P. M. Harmans, J. G. Williamson, H. van Houten, C. W. J. Beenakker, C. T. Foxon, and J. J. Harris, Phys. Rev. B **39**, 8040 (1989).

[14]N. K. Patel, L. Martin-Moreno, M. Pepper, R. Newbury, J. E. F. Frost, D. A. Ritchie, G. A. C. Jones, J. T. M. B. Janssen, J. Singleton, and J. A. A. J. Perenboom, J. Phys. Condens. Matter **2**, 7247 (1990).

[15]N. K. Patel, J. T. Nicholls, L. Martin-Moreno, M. Pepper, J. E. F. Frost, D. A. Ritchie, and G. A. Jones, Phys. Rev. B **44**, 13 549 (1991).

[16]L. I. Glazman and A. V. Khaetskii, Europhys. Lett. **9**, 263 (1989).

[17]L. Martin-Moreno, J. T. Nicholls, N. K. Patel, and M. Pepper, J. Phys. Condens. Matter **4**, 1323 (1992).

[18]E. Castaño and G. Kirczenow, Phys. Rev. B **41**, 3874 (1990).

[19]G. S. Lent, S. Sivaprakasam, and D. J. Kirkner, Solid State Electron. **32**, 1137 (1989).

[20]S. Bandyopadhyay, S. Chaudhuri, B. Das, and M. Cahay, Superlatt. Microstruct. **12**, 123 (1992).

[21]Hongqi Xu, Phys. Rev. B **47**, 9537 (1993).

[22]Hongqi Xu, Zhen-Li Ji, and K.-F. Berggren, Superlatt. Microstruct. **12**, 237 (1992).

[23]In models that consider an adiabatic change in geometry, the edges of the conductance plateaus may also be identified by the peaks in $\partial G/\partial V_{sd}$, the derivative of the differential conductance G with respect to applied source-drain voltage V_{sd}, or by the peaks in $\partial G/\partial V_g$, the derivative of the differential conductance G with respect to gate voltage V_g. See, for example, A. M. Zagoskin, Pis'ma Zh. Eksp. Teor. Fiz. **52**, 1043 (1990) [JETP Lett. **52**, 435 (1990)], and Ref. 15.